Available online at www.sciencedirect.com
ScienceDirect
Trans. Nonferrous Met. Soc. China 21(2011) 236−242
Transactions of Nonferrous Metals Society of China
www.tnmsc.cn

Solidification process of conventional superalloy by confocal scanning laser microscope

MIAO Zhu-jun[1], SHAN Ai-dang[1], WANG Wei[2], LU Jun[3], XU Wen-liang[3], SONG Hong-wei[3]

1. School of Materials Science and Engineering, Shanghai Jiao Tong University, Shanghai 200240, China;
2. School of Mechanical and Power Engineering, East China University of Science and Technology, Shanghai 200237, China;
3. Baosteel Research Institute, Baoshan Iron and Steel Co., Ltd., Shanghai 201900, China

Received 6 April 2010; accepted 28 October 2010

Abstract: The solidification process of a conventional superalloy, IN718, was investigated by confocal scanning laser microscope (CSLM). The liquid fraction during solidification was obtained as a function of real time and temperature in reference with the *in-situ* observation. The characteristics of $L\rightarrow\gamma$ transformation were analyzed and the γ growing rate of each stage was also calculated. Scheil equation was employed to predict the segregation behavior, and the predict results are in consistence with the experimental results. As a result, the confocal scanning laser microscope shows a great potential for solidification process research.
Key words: IN718 alloy; solidification; *in-situ*; confocal scanning laser microscope; segregation

1 Introduction

IN718 alloy is a kind of precipitation-strengthened wrought superalloy widely used in the gas turbine industry[1−2], Because of its excellent balance of properties and reasonable cost, IN718 is accounting for more than 50% of commercial superalloy productions in the world[3]. With the development of land-based power generation and aircraft propulsion, scaling-up of components has become the necessity. The size of IN718 ingot produced by VIM-ESR-VAR triple melting has increased dramatically over the past 10 years in response to market demands[4−6]. However, the solute segregation problem, mainly niobium segregation, is a big obstacle for producing large size IN718 ingots. Particularly, some macro-segregations defects such as freckles and white spots formed during the solidification process will lead to entire failure for the whole ingot. So, the driving force for studying the solidification behavior of IN718 superalloy still exists.

In the previous studies, a lot of methods have been employed to investigate the solidification behavior of IN718 superalloy, including DTA, high temperature freezing and computational modeling. For example, KNOROVSKY et al[7] obtained transformation temperatures by DTA and presented a solidification diagram for an idealized IN718. WANG et al[8] used high temperature freezing method to keep the initial liquid state of alloy, expecting to analyze original solidification process. Thermo-calc and JMatPro software were also employed to calculate the liquid composition and equilibrium diagrams of IN718. These methods provide a variety of valuable solidification information and can be used to predict segregation during melting or casting[8−9].

Recently, confocal scanning laser microscope (CSLM) offers a great capability for real-time and continuous observation of phase transformation at high temperatures. This method has already been adopted for study of solidification process of low carbon steel[10−11], stainless steel[12] and metallic glass[13]. Therefore, it is of great interest to perform an *in-situ* observation of solidification process of IN718 superalloy. Furthermore, the microstructure and segregation behavior of the solidified CSLM sample are characterized in this study, in comparison with the simulated results using Scheil equation.

Foundation item: Project(08dj1400402) supported by the Major Program for the Fundamental Research of Shanghai Committee of Science and Technology, China
Corresponding author: SHAN Ai-dang; Tel: +86-21-54747441; Fax: +86-21-54748974; E-mail: adshan@sjtu.edu.cn
DOI: 10.1016/S1003-6326(11)60704-8

2 Experimental

It is noticed that the detailed characteristics of CSLM have been described in the previous studies[10]. The shallow undulation of sample surface caused by phase transformation and small difference of reflectivity between transforming phases could be sensitively detected by CCD image sensor of CSLM. And it is possible to observe phase transformation process at high temperatures up to 1 600 °C[11]. Simultaneously, the real-time pictures were recorded on hard discs at a rate of 30 frames per second. Fig.1 shows the basic components of a confocal scanning laser microscope (1LM21H from Lasertec Corporation), which includes microscope, metallurgy furnace, monitor, computer, protective air system, vacuum pump and circular water system. For this model, magnifications up to 2 450 times are available, using a He-Ne laser with a wavelength of 633 nm.

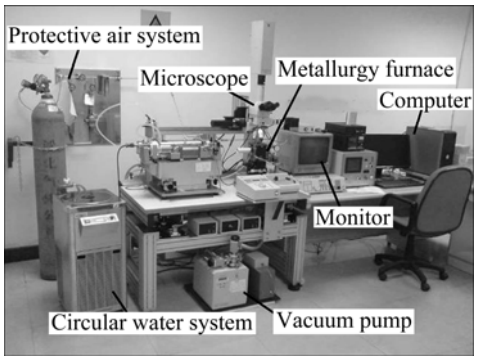

Fig.1 Components of confocal scanning laser microscope

The IN718 superalloy used in this study was prepared by 10 kg-vacuum induction furnace and chemical compositions (mass fraction, %) of the IN718 are listed in Table 1. Samples for CSLM study were machined into a round column shape (4 mm in diameter and 3 mm in height). Before the *in-situ* observation, the samples were mirror polished and put into an alumina crucible. Then, the crucible was placed into the heating position of metallurgy furnace with thermocouple attached. After evacuating the gases in the furnace chamber by vacuum pump, ultra pure argon (99.999%) was purged into the chamber continuously in order to avoid oxidation of the sample surface.

Table 1 Chemical compositions of IN718 superalloy (mass fraction, %)

C	P	B	Al	Ti
0.05	0.004	0.0011	0.52	1.00
Mo	Nb	Cr	Ni	Fe
3.10	5.33	19.5	53.0	Bal.

Since the purpose of this investigation was to explore the solidification process, DSC test was conducted to identify the temperatures of phase transformation during solidification. Fig.2 shows that the primary crystallization (first peak) takes place at 1 337.4 °C. The second peak and third peak were associated with the MC carbide and the Laves phase. According to the above analysis, the CSLM sample was heated to 1 400 °C in 8 min, and then held for a further 5 min at 1 400 °C before cooling at 100 °C /min to 1 100 °C. Finally, the furnace was power-off at 1 100 °C to let the sample cool to room temperature. The accuracy of measured temperatures is a key issue in CSLM observation. According to the work of SHIBATA and EMI[14], almost no difference was found between sample surface and crucible bottom when the temperature was below 1 100 K. But as the temperature increased, the difference gradually appeared. When the measured temperature was 1 670 K at the bottom of crucible, the actual temperature at the center of sample surface was 1 650 K. Here, the difference between actual temperatures and measured temperature was treated as systematic error and was not taken into consideration.

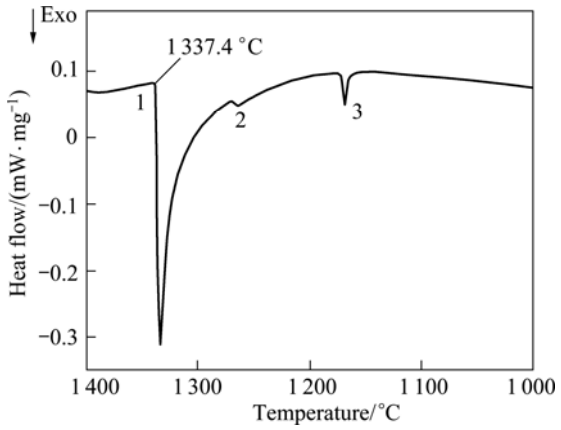

Fig.2 DSC curve of test alloy

Afterwards, the OM and SEM samples were prepared by mechanical polishing and electro-etching in a mixture solution of 11% (volume fraction) hydrochloric acid, 33% nitric acid and 56% glycerin at a voltage of 6 V for 8 s. The solidified microstructures were examined by scanning electron microscope (SEM: Tescan-Vega) equipped with an energy dispersive X-ray micro-analyzer (EDX: Bruker).

3 Results and discussion

3.1 Solidification process

Fig.3 illustrates the solidification process of IN718 alloy at a cooling rate of 100 °C/min, which was obtained by using CSLM. The variations of temperature

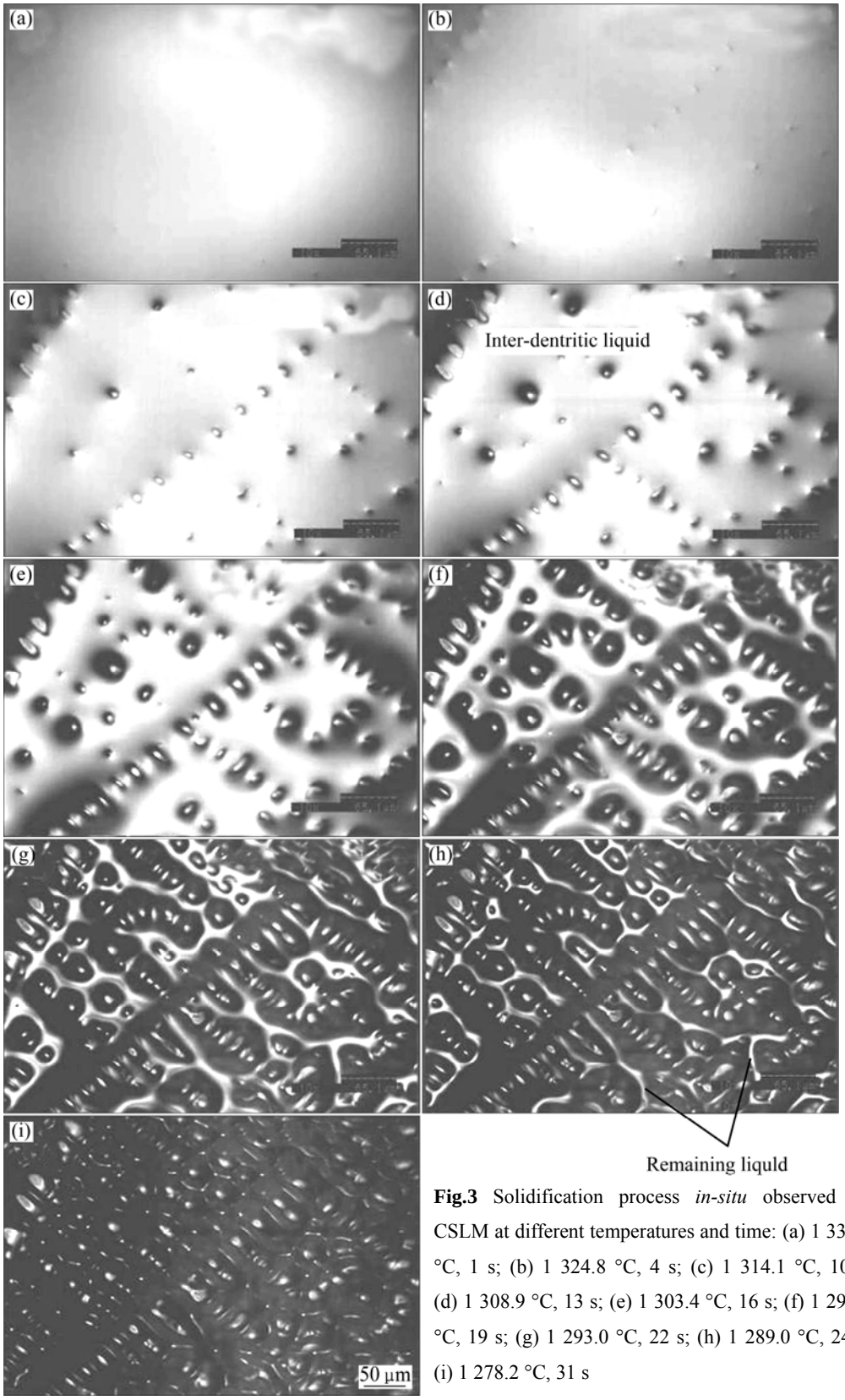

Fig.3 Solidification process *in-situ* observed by CSLM at different temperatures and time: (a) 1 331.1 °C, 1 s; (b) 1 324.8 °C, 4 s; (c) 1 314.1 °C, 10 s; (d) 1 308.9 °C, 13 s; (e) 1 303.4 °C, 16 s; (f) 1 298.2 °C, 19 s; (g) 1 293.0 °C, 22 s; (h) 1 289.0 °C, 24 s; (i) 1 278.2 °C, 31 s

and real time are also displayed on the continuously recorded pictures. In the previous study, the crucible provides a favorable site for heterogeneous nucleation in AISI304 stainless steel[12]. Similarly, seen from Fig.3, it is inferred that the solidification of IN718 alloy has commenced below the surface of the opaque melt and is gradually being revealed on the melt surface. With the decrease of temperature, the solid-liquid interface is

moving heading to the inter-dendritic region and areas of liquid pool become smaller and smaller. But, some remaining liquid still exists in the final solidification stage of primary crystallization. It is believed that these remaining liquid areas are the most segregated regions and severe segregation also leads to the reduction of solidifying temperatures for IN718 superalloy. Therefore, it is normal to find that remaining liquid cannot solidify for a long time in the CSLM observation. Unfortunately, the formation of Laves phase in the inter-dendritic region cannot be observed because of the equipment capability.

We can see from the previous analysis that it is reasonable to acquire the liquid volume fraction on the free surface by calculating the liquid area fraction of each picture recorded in CSLM observation. Here, AutoCAD software was used to calculate the liquid volume fraction and yield the relationship between liquid volume fraction and time as well as liquid volume fraction and temperature. Avrami equation[15] was utilized for fitting the above curves and results are available in Fig.4.

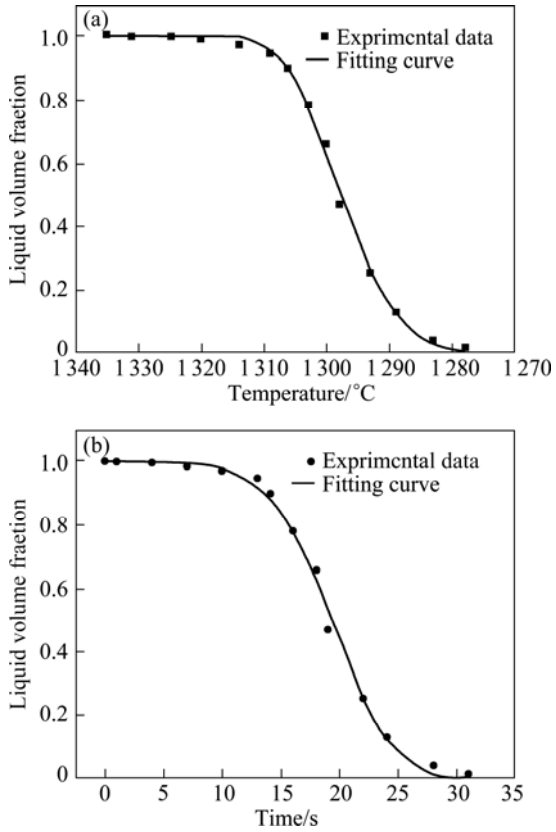

Fig.4 Fitted curves of liquid volume fraction as function of temperature (a) and time (b)

For the liquid fraction (f_L) as a function of temperature (θ, °C):

$$f_L = 1 - \exp[-2.21\times10^{-7}(\theta - 1\ 270)^{4.5}] \quad (1)$$

In reference with Fig.3(a), it is known that the transition temperature from liquid to γ is 1 331.1 °C. Moreover, the applied cooling rate was 100 °C /min, which means that time (t, s) is dependence of temperature (θ, °C) as the following relationship:

$$\theta = 1331 - \frac{5}{3}t \quad (2)$$

So, the liquid fraction as a function of time can be obtained:

$$f_L = 1 - \exp[-2.21\times10^{-7}(61 - \frac{5}{3}t)^{4.5}] \quad (3)$$

It is obviously seen from Fig.4 that there are three stages for $L\rightarrow\gamma$ solidification from the given curves. They are here named as initial stage, stable stage and last stage, respectively. After linear fitting of three stages, comparison can be made to demonstrate the characteristic of each stage, as shown in Fig.5. Firstly, in the initial stage of $L\rightarrow\gamma$ solidification process, the solutes segregated little by little in the front edge of L/γ interface, resulting in the reduction of liquidus temperature. The $L\rightarrow\gamma$ phase transformation can only happen with the further decrease of temperature. So, γ growing rate is 0.004 s^{-1} at this stage. Secondly, $L\rightarrow\gamma$ transformation goes to a more stable stage. At this stage, the L/γ interface is moving in a stationary speed and the γ growing rate is 0.083 s^{-1}, almost 20 times that of initial stage. Finally, when the remaining liquid becomes less, the transformation comes to the last stage. The segregated large size solutes (such as Nb and Mo) in the remaining liquid cannot diffuse across the L/γ interface, so the concentration of segregated element is rising dramatically, which leads to the low speed growth again. At the last stage, γ growing rate is 0.016 s^{-1}.

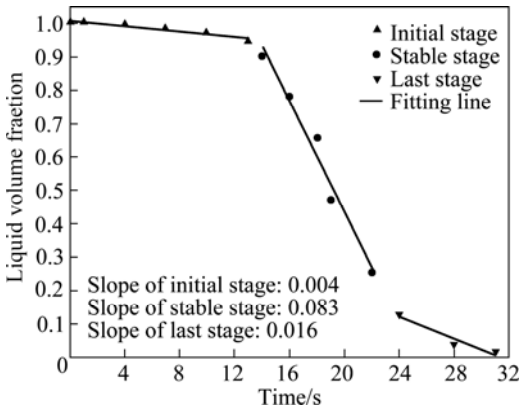

Fig.5 Three stages for $L\rightarrow\gamma$ transformation

3.2 Microstructure analysis on solidified CSLM sample

Fig.6(a) shows the typical microstructure of solidified CSLM sample. It can be seen that a lot of white blocky Laves phase exist in the inter-dendritic

region. MC carbides are also detected around the Laves phase, also in the inter-dendritic region. Figs.6(b)−(d) present the EDX spectra of three different spots and related chemical compositions are listed in Table 2. The results indicate that Nb and Mo are severely enriched in the Laves phase. On the contrast, Nb and Mo are obviously poor in the dendrite core. MC carbide is mainly composed of two elements: Nb and Ti.

In order to verify the element segregation behavior along the Laves phase, composition distribution along marked line in Fig.7(a) is obtained by EDX. From Fig.7(b), it is clear that Cr and Fe segregate into the dendrite core while Nb and Mo tend to accumulate in the inter-dendritic region. Additionally, three parts can be divided according to the elements composition profile: Laves phase, segregation zone and dendrite core. It is noted that the Laves phase contains 28.2 % Nb (mass fraction), almost five times nominal composition of the IN718. Compared with Laves phase, Nb content shows a falling tendency in segregation zone but still be enriched at a high level. However, only 3.4% Nb (mass fraction) is remained in the dendrite core, which is much lower than nominal composition of the alloy. Similarly, Mo shares the same segregation pattern with Nb. The results of EDX examinations indicate that serious segregation happens in solidified CSLM sample, especially for Nb.

3.3 Segregation simulation using Scheil equation

Following the above study, it is noted that a lot of strengthening elements are enriched in inter-dendrite areas. So, segregation modeling is very valuable for predicting the compositions during solidification. In this study, we use a simple model, known as Scheil equation[16], which is widely used nowadays for its simplicity and capability in dealing with solidification research. Assuming there is no solid state

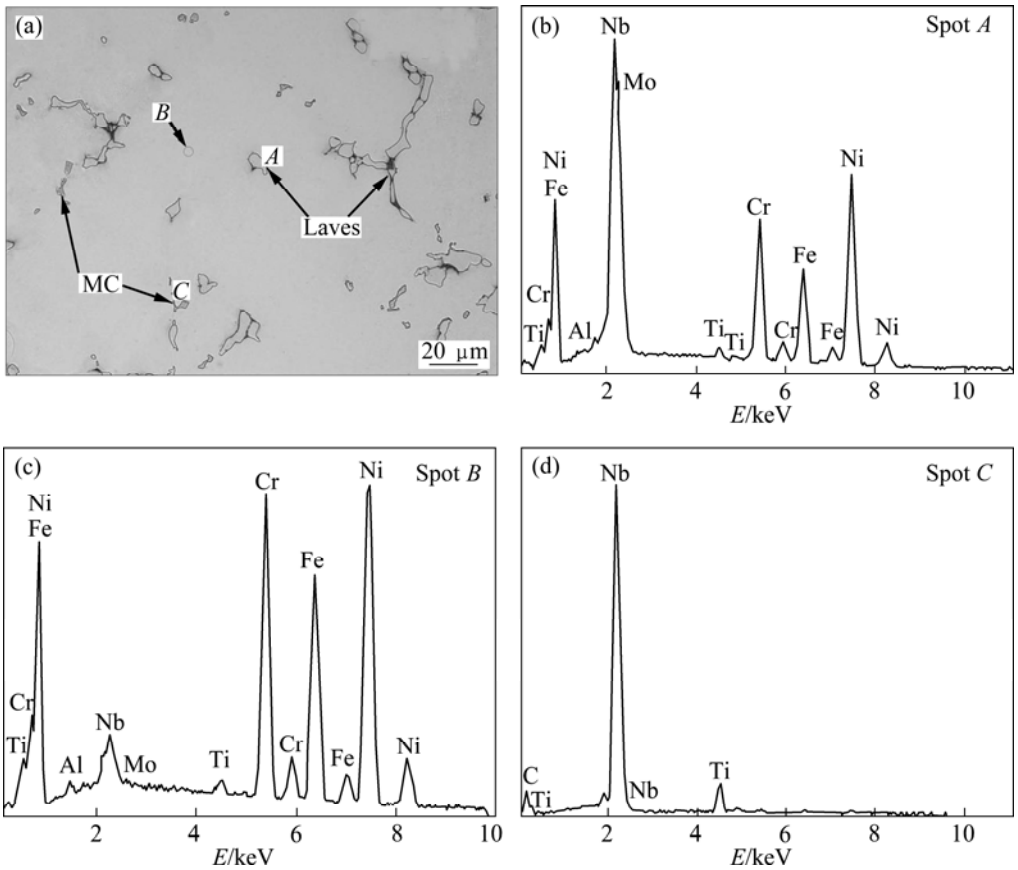

Fig.6 Microstructure of solidified sample after CSLM experiment (a) and EDX spectra of Laves phase (b), dendrite core (c) and MC carbide (d)

Table 2 Chemical compositions of representative locations in solidified CSLM sample (mass fraction, %)

Location	Ni	Cr	Fe	Nb	Mo	Ti	Al
Spot *A*	35.17	14.48	13.53	28.23	7.01	0.98	0.6
Spot *B*	52.95	21.01	18.89	3.51	2.43	0.71	0.5
Spot *C*	−	−	−	92.39	−	7.61	−

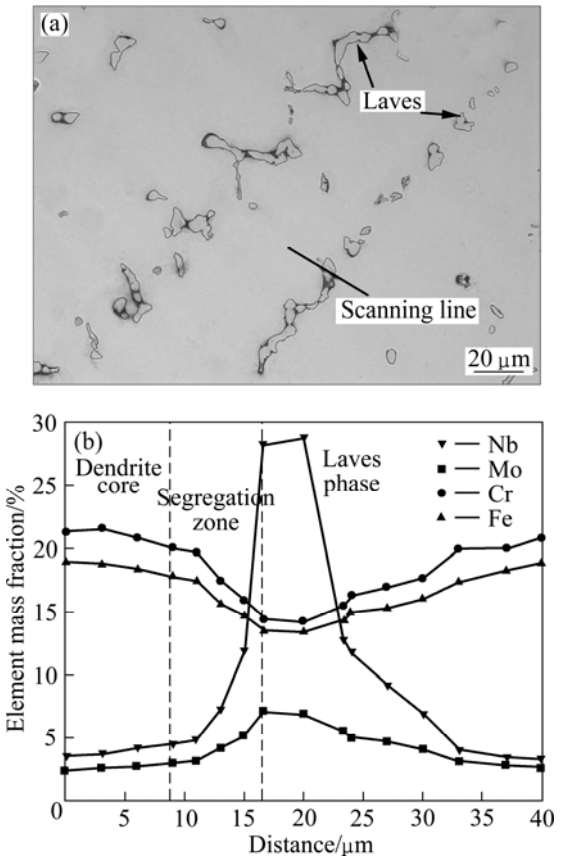

Fig.7 Composition profile along Laves phase by EDX: (a) EDX scanning line; (b) Element mass fraction

diffusion and no dendritic side branching, and thermodynamic equilibrium is maintained at the moving solid/liquid interface during solidification[8], the alloying element composition profile can be described by the following relationship:

$$C_S = k_0 C_0 (1 - f_S)^{k_0 - 1} \quad (4)$$

where C_S (mass fraction, %) is the instantaneous solid composition forming at the correspondent solid fraction (f_S); k_0 is the distribution coefficient for the element; C_0 is the nominal element mass fraction of IN718 superalloy.

The value of k_0 can be obtained by measuring the concentration of element (C_S) at $f_S = 0$. The results listed in Table 3 indicate that k_0 of Nb or Mo is less than unity while k_0 of Cr or Fe is greater than unity. Meanwhile, Cr and Fe share the similarity for segregation behavior.

Fig.8 shows the simulated variation of C_S for four elements according to the Scheil equation. In the calculation process, it is defined that solidification ends when the solid fraction (f_S) reaches 0.99. As a result, it is found that with the proceeds of solidification, Nb and Mo show a rising tendency while Cr and Fe show a falling tendency. Compared with previous EDX results, Scheil equation can be successfully applied to describing the segregation profile in IN718. Especially for Mo, Cr and Fe, the simulated results perfectly match with the experimental results. As for the most segregated element (Nb), there is a little difference in the Laves phase between simulated results and experimental results.

Table 3 Distribution coefficient of elements in IN718 superalloy

Nb	Mo	Cr	Fe
0.64	0.80	1.09	1.08

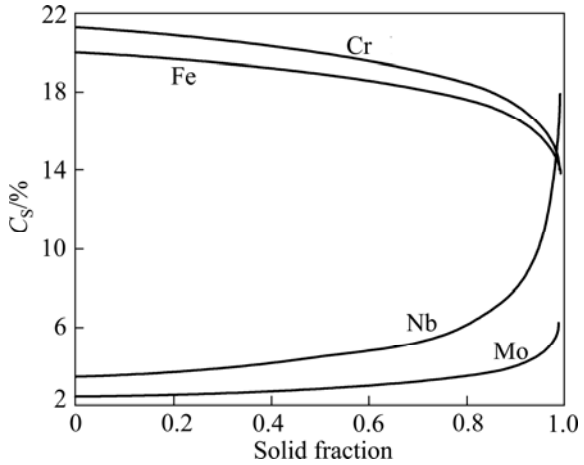

Fig.8 Variation of C_S during solidification

4 Conclusions

1) The confocal scanning laser microscope offers unique opportunity and exhibits great potential for the research of solidification process. According to the *in-situ* observation results, the liquid fraction (f_L) during solidification can be expressed as a function of temperature (θ, °C).

2) Three stages can be defined for $L \rightarrow \gamma$ transformation of IN718 alloy: initial stage, stable stage and last stage. When solidified at the cooling rate of 100 °C /min, the γ growing rates of three stages are 0.004 s^{-1}, 0.083 s^{-1} and 0.016 s^{-1}, respectively.

3) The segregation behavior of the solidified CSLM sample is simulated by Scheil equation, which is in good agreement with the experimental result.

Acknowledgments

The authors would like to thank Dr SUN Wen-ru from Institute of Metal Research for kindly help and useful discussions. CSLM observations were conducted at Advanced Technology Division of Baosteel Research Institute, under the supervision of Mr. WANG Chen-quan.

References

[1] GEN L, ZHENG Z, NA Y, PARK N. Effect of thermal exposure on precipitation behavior and hardness of alloy 718 [J]. Trans Nonferrous Met Soc China, 2000, 10(3): 340−344.

[2] HONG S, CHEN W, WANG T. A diffraction study of the γ'' phase in INCONEL 718 superalloy [J]. Metallurgical and Materials Transactions A, 2001, 32: 1887−1901.

[3] DECKER R. The evolution of wrought age-hardenable superalloys [J]. JOM, 2006, 58: 32−36.

[4] CARTER W, JONES R. Nucleated casting for the production of large superalloy ingots [J]. JOM. 2005, 57: 52−57.

[5] MALARA C, RADAVICH J. Alloy 718 large ingots studies [C]//Proc Superalloys 718, 625, 706 and Derivatives. PA, USA: TMS, 2005: 25−34.

[6] SCHWANT R, THAMBOO S, YANG L, MORRA M. Extending the size of alloy 718 rotating components [C]//Proc Superalloys 718, 625, 706 and Derivatives. PA, USA: TMS, 2005: 15−24.

[7] KNOROVSKY G, CIESLAK M, HEADLEY T, ROMIG A, HAMMETTER W. Inconel 718: A solidification diagram [J]. Metallurgical and Materials Transactions A, 1989, 20: 2149−2158.

[8] WANG L, DONG J, TIAN Y, ZHANG L. Microsegregation and Rayleigh number variation during the solidification of superalloy Inconel 718 [J]. Journal of University of Science and Technology Beijing, 2008, 15: 594−599.

[9] SAUNDERS N, GUO Z, MIODOWNIK A, SCHILLE J. Modelling the material properties and behaviour of Ni-Fe-based superalloys [C]//Proc Superalloys 718, 625, 706 and Derivatives. PA, USA: TMS, 2005: 571−580.

[10] YIN H, EMI T, SHIBATA H. Determination of free energy of δ-ferrite/ γ-austenite interphase boundary of low carbon steels by *in-situ* observation [J]. ISIJ International, 1998, 38: 794−801.

[11] YIN H, EMI T, SHIBATA H. Morphological instability of δ-ferrite/ γ-austenite interphase boundary in low carbon steels [J]. Acta Materialia, 1999, 47: 1523−1535.

[12] LIANG G, WAN C, WU J, ZHU G, YU Y, FANG Y. In situ observation of growth behavior and morphology of delta-ferrite as function of solidification rate in an AISI304 stainless steel [J]. Acta Metallurgica Sinica (English Letters), 2006, 19: 441−448.

[13] KIM J, KIM S, INOUE A. In situ observation of solidification behavior in undercooled Pd-Cu-Ni-P alloy by using a confocal scanning laser microscope [J]. Acta Materialia, 2001, 49: 615−622.

[14] SHIBATA H, EMI T. In situ high-temperature behavior of metal precipitates and inclusions by confocal scanning laser microscope [J]. Materia Japan, 1997, 36: 809−813.

[15] HU Geng-xiang, CAI Xun. The fundamental of materials science [M]. Shanghai: Shanghai Jiao Tong University Press, 2000. (in Chinese)

[16] FLEMINGS M. Solidification processing [M]. New York: McGraw-Hill, 1974.

利用共聚焦扫描激光显微镜观察一种常见高温合金的凝固过程

缪竹骏[1], 单爱党[1], 王 威[2], 卢 俊[3], 徐文亮[3], 宋洪伟[3]

1. 上海交通大学 材料科学与工程学院, 上海 200240; 2. 华东理工大学 机械与动力工程学院, 上海 200237;
3. 宝山钢铁股份有限公司 宝钢研究院, 上海 201900

摘 要：利用共聚焦扫描激光显微镜直接观察一种常见高温合金(IN718)的凝固过程。根据动态原位观察结果，凝固过程中的液相体积分数可以表示为时间或温度的函数，分析 $L\rightarrow\gamma$ 的凝固过程得到不同阶段的 γ 生长速率。利用 Scheil 方程对凝固过程中元素的偏析行为进行模拟，计算结果与原位观察结果相吻合。共聚焦扫描激光显微镜作为研究合金凝固行为的工具极具潜力。

关键词: IN718 合金; 凝固; 原位; 共聚焦扫描激光显微镜; 偏析

(Edited by LI Xiang-qun)